VOL. X, NO. X, XXXXXXXX ISSN 1819-6608
ARPN Journal of Engineering and Applied Sciences


www.arpnjournals.com

INVERSE KINEMATICS ANALYSIS OF A 5-AXIS RV-2AJ ROBOT MANIPULATOR

Mohammad Afif Ayob[1a], Wan Nurshazwani Wan Zakaria[1b], Jamaludin Jalani[2c], Mohd Razali Md Tomari[1d]
[1]ADvanced Mechatronics Research Group (ADMIRE), Faculty of Electrical and Electronic Engineering, Universiti Tun Hussein Onn Malaysia, 86400 Parit Raja, Batu Pahat, Malaysia.
[2]Department of Electrical Engineering Technology, Faculty of Engineering Technology, Universiti Tun Hussein Onn Malaysia, 86400 Parit Raja, Batu Pahat, Malaysia.
E-Mail: [a]mohammadafifayob@gmail.com, [b]shazwani@uthm.edu.my, [c]jamalj@uthm.edu.my, [d]mdrazali@uthm.edu.my

ABSTRACT
This paper presents the inverse kinematics analysis of the five degree of freedom (DOF) Mitsubishi Melfa RV-2AJ industrial robot. The proposed method is used specifically for controlling the z-axis Cartesian position. The kinematics problem is defined as the transformation from the robot's end-effector Cartesian space to the joint angle of the robotic arms. An analytical solution using trigonometry illustration is presented to describe the relation between the position of the robot end-effector to each of the robot joints. Several lab experiments to validate the established kinematics equations have been conducted. In this study, the developed kinematics solutions were found to be accurate to approximately 99.83% compared to the real robot. These findings have significant implication for developing a kinematic simulation model that can be used to evaluate position and force control algorithm.

Key words: Inverse kinematics • Mitsubishi Melfa RV-2AJ • Pythagoras's theorem •

INTRODUCTION

Robotics technology is at the convergence of diverse branch of knowledge that one must realize to successfully express the motion of complex robotic systems. At present, incorporation of human in the process is fundamental for a rapid setup, programming and robot system maintenance. Therefore, before any robotic system is associated to a specific workplace, a simulation approach is often needed to provide deep understanding upon the control framework and its behavior. By simulating the robot and its environment, the human can consistently improve the overall system, reduce the build cost, and eliminate the risks the robot might exerts on the user.

The Mitsubishi RV-2AJ robot as shown in Figure 1 has been chosen as a case study as it thecnically offers the best performance as a small, compact and powerful articulated-arm robot in its class. The robot operates using AC servomotors that can produce a maximum speed of 2100 mm/s with a repeatability of ±0.02 mm. The high precision motors with integrated absolute position encoders consistently ensure reliable and maintenance-free operation (Esa, Ibrahim, Mustaffa, & Majid, 2011).

The maximum payload of the robot is rated at 2 kg and thus is exceptionally sufficient for low payload handling, placing and separating small parts. Another prominent applications that are worth mentioning include quality control and handling samples in medical and other laboratories. Since the robot is able to cover horizontal motion of up to 410 mm (with the gripper pointed downwards), it is also ideal for applications where a small and compact robot needs to be installed directly next to or even in any automated system.

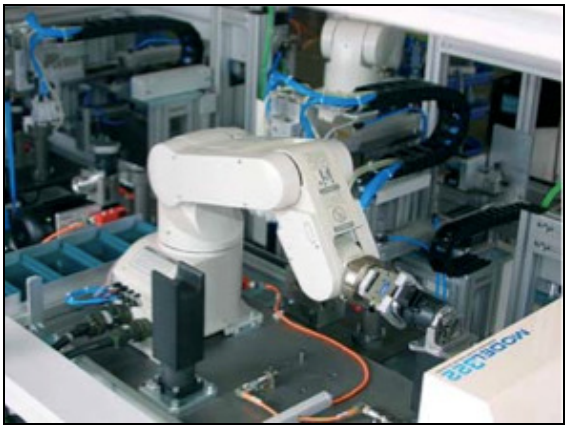
Figure 1: RV-2AJ at work in cramped quarters. (Mitsubishi Electric, 2009).

Taking into consideration the way the five jointed robot arm of the RV-2AJ is engineered, the mechanical structure is designated as anthropomorphic articulate (having human-like characteristics). Every single joint has one freedom of rotation around its own axis. The motion axes for the model are assigned with their own nomenclature as follows: base rotation for Joint 1, shoulder rotation for Joint 2, elbow rotation for Joint 3, wrist pitch for Joint 4, and wrist roll for Joint 5. Figure 2 shows the assigned naming convention.

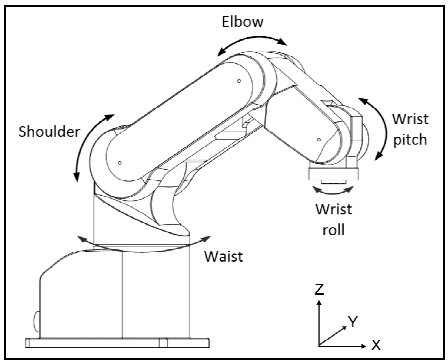

Figure 2: RV-2AJ robot arm joints.

Table 1 lists the maximum working envelope for each joint of the robotic arm while Table 2 lists the link distance between those joint. Each link has its own range limitation allocated by the manufacturer so that the arm will not move beyond the range and thus damaging the servo motor. The complete dimensions of the link frames, the distance between the joints and the robot work envelope are given in Figure 3.

Table 1: Rotation range for RV-2AJ. (Mitsubishi Electric, 2002).

Joint	Angle Range
1: Waist rotation	-150° to +150°
2: Shoulder rotation	-60° to +120°
3: Elbow rotation	-110° to +120°
4: Wrist pitch	-90° to +90°
5: Wrist roll	-200° to +200°

Table 2: Link distance for RV-2AJ. (Mitsubishi Electric, 2002).

Link	Distance
1: Waist to shoulder	300 mm
2: Shoulder to elbow	250 mm
3: Elbow to wrist	160 mm
4: Wrist to end	72 mm

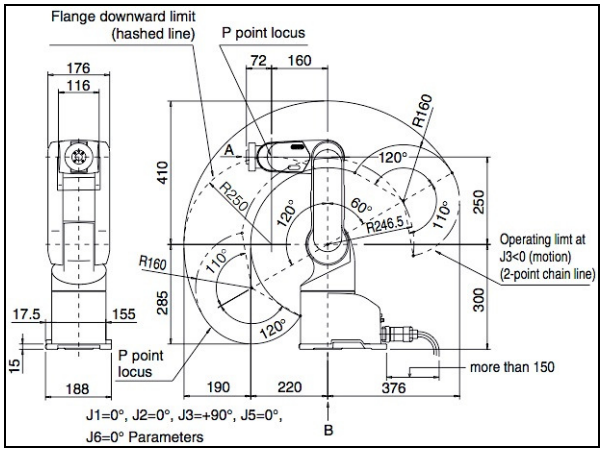

Figure 3: Dimensions of RV-2AJ robot. (Mitsubishi Electric, 2002).

Inverse kinematics of RV-2AJ robot

The inverse kinematics study consists of determining the joint angles of a robot from its specified end-effector Cartesian position. The analysis of this inverse kinematics for the robot mechanical structures is vital to realize the mechanical system, allowing the development of further studies and applications.

In the past, previous researchers have established different method for developing inverse kinematics of the RV-2AJ robot than the one being discussed in this paper. Such is by implementing an iterative algorithm based on Jacobian transpose matrix (Haklidir & Tasdelen, 2009). However, for no reasonable justification, the kinematic model was developed only up to the first three joints (instead of five) and no experiments result were showed at all to verify the accuracy of the model. As a result of the limited DOF and the unknown accuracy, the position of the end-effector will always be ambiguous. Several other researches have also developed the inverse kinematics solution for the RV-2AJ, but again the accuracy of the models were not proven by any approach (Coman, Balan, Donca, & Verdeş, 2011; Coman, Stan, Manic, & Balan, 2009; Šljivo, 2013). On that account, this paper addresses this matter thoroughly with comparison to experimental results in order to validate the accuracy of the developed model. In addition, considering that the proposed method in this paper is limited to just controlling the z-axis Cartesian position of the robot, the process is much simpler and straightforward to develop compared to other conventional method from previous researchers.

Pythagoras's theorem in inverse kinematics problem

In order to solve the inverse kinematics problem for the 5-axis RV-2AJ robot using Pythagoras's theorem, a conclusion has been made in which that the solution is not applicable for the wrist roll of the robot. This is because the rotation of the wrist roll does not have any influence on the end-effector Cartesian position. Therefore, the joint angle of the wrist roll is not considered.

Referring to the top view of the robot as shown in Figure 4, the waist joint angle of θ_1 can be easily resolved. Additionally, it can be seen that wherever the robot moves in any Cartesian position that is permissible for the robot, the waist joint angle could always be calculated by using the same technique that will be discussed in this section.

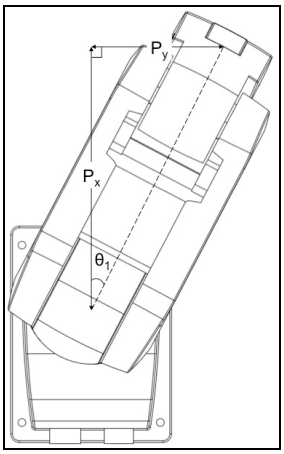

Figure 4: Determining waist angle at joint 1.

Since the robot posture resulted in Figure 4 produces a right-angled triangle that involves the angle at first joint, the following Pythagoras's theorem applies:

$$\tan \theta_1 \quad \frac{P_y}{P_x} \tag{1}$$

Hence, $\theta_{\_}$ can be calculated as follows:

$$\theta_{\_} \quad \tan^{-1}\left(\frac{P_y}{P_x}\right) \tag{2}$$

Before the same theorem is applied to identify the subsequent joint angles of the robot, the initial condition of the wrist pitch has to be configured as shown in Figure 5 so that the wrist pitch is always perpendicular to the ground level at all times during the experiments. To achieve the required setting, both the elbow and the wrist pitch were inclined at +90° while the shoulder is at 0° respectively.

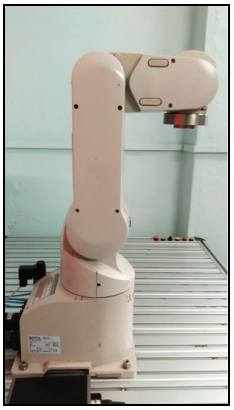

Figure 5: RV-2AJ robot with wrist pitch at vertical position.

Figure 6 shows an example position to acquire the shoulder joint angle of θ_2 to θ_4 of the robot. The law of sine will be used in this section as the following equation:

$$\frac{a}{\sin \theta_A} \quad \frac{b}{\sin \theta_B} \quad \frac{c}{\sin \theta_C} \tag{3}$$

The length of c is obtained by using the known sides of the triangle using relevant Pythagoras's theorem as follows:

$$c \quad \sqrt{Px^2 + |300 \quad (Pz + 72)|^2} \tag{4}$$

The law of cosine relates the lengths of the sides of a triangle to the cosine of one of its angles. Hence we can get θ_C:

$$c^2 \quad a^2 + b^2 \quad 2ab\cos\theta_C \tag{5}$$

$$\theta_C \quad \cos^{-1}\left(\frac{a^2 + b^2 \quad c^2}{2ab}\right) \tag{6}$$

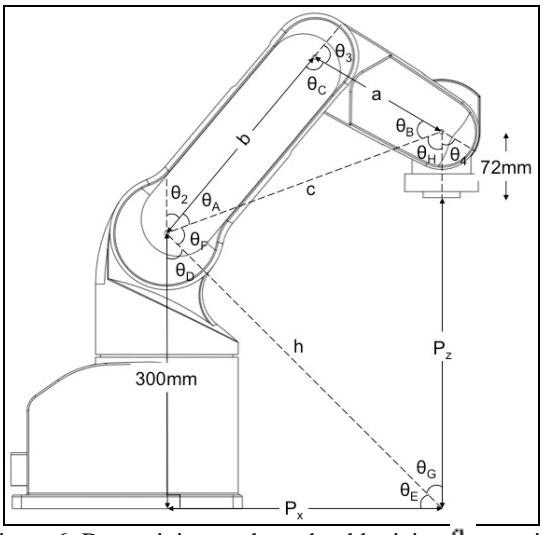

Figure 6: Determining angle at shoulder joint, θ_2 to wrist joint, θ_4.

Since the joint angle of each link of the robot is based on the previous link inclination, hence:

$$\theta_3 \quad 180 \quad \theta_C \tag{7}$$

Substitute the calculated θ_C to equation (3) to acquire θ_A and θ_B:

$$\theta_A \quad \sin^{-1}\left(\frac{a}{c}\sin\theta_C\right) \tag{8}$$

$$\theta_B \quad \sin^{-1}\left(\frac{b}{c}\sin\theta_C\right) \tag{9}$$

Next, to solve the following triangle, we get:

$$\theta_E \quad \tan^{-1}\left(\frac{300}{Px}\right) \tag{10}$$

Since both θ_D and θ_E are within their right-angled triangle, this yields to:

$$\theta_D \quad \theta_E \quad 90 \quad \theta_E \tag{11}$$

For the next section of the triangle, we get:

$$\frac{c}{\sin\theta_C} \quad \frac{h}{\sin\theta_H} \quad \frac{Pz + 72}{\sin\theta_F} \tag{12}$$

with:

$$h \quad \sqrt{300^2 + Px^2} \tag{13}$$

Calculating θ_F from (12), we have:

$$\theta_F \quad \sin^{-1}\left(\frac{Pz + 72}{c}\sin\theta_C\right) \tag{14}$$

Consequently, the remaining joint angles of θ_2 and θ_4 can be obtained as follows:

$$\theta_2 \quad 180 \quad \theta_A \quad \theta_D \quad \theta_F \tag{15}$$

$$\theta_H \quad 180 \quad \theta_C \quad \theta_F \tag{16}$$

$$\theta_4 \quad 180 \quad \theta_B \quad \theta_H \tag{17}$$

Results and analysis

The inverse kinematics of the RV-2AJ robot has been implemented and simulation study has been performed using the MATLAB program. To find out the angle at joint 1, several random positions of the x-axis position, *Px* and the y-axis position, *Py* were taken. For experimental results of finding the joint angles at joint 2 to joint 4, the Cartesian coordinates for the end-effector of the robot were set in a way that *Px* is fixed at 302.45 mm while *Py* is fixed at 0 mm at all time. However, it should be noted that the applied inverse kinematics method is still applicable when there are any movements anywhere in these axes. The experiment variable, which is the z-axis position, *Pz* of the robot end-effector changes from 397.35 mm down to 207.36 mm with 10 mm reduction (±1-3 mm) for each sample taken.

The desired Cartesian coordinates of the robot were manually controlled via the teach pendant and the joint angles of the robot were directly obtained from its display panel. Comparison between simulation and experiment results are analyzed in this section. In order to fully validate the workability of the developed inverse kinematics method, data taken from the experiments were categorized into three possible configurations.

Determining θ_1

To determine the first joint angle, θ_1 of the RV-2AJ robot, the end-effector was placed in different Cartesian positions such as in Figure 4. Comparison for both simulation and experimental results were recorded in Table 3. The error produced is found to be approximately 0.196%.

Table 3: Comparison between simulation and experimental results for determining θ_1.

No. of test	Px (mm)	Py (mm)	Simulation (degree)		Experiment (degree)		Difference (degree)	Error (%)
1	-0.02	0	θ_1	0	θ_1	0	0	0
2	224.52	156.22	θ_1	34.83	θ_1	34.83	0	0
3	63.37	14.74	θ_1	13.0943	θ_1	13.09	-0.0043	-0.43
4	50.73	56.5	θ_1	48.0801	θ_1	48.08	-0.0001	-0.01
5	247.56	-93.02	θ_1	-20.594	θ_1	-20.59	0.004	0.4
6	7.04	-140.77	θ_1	-87.137	θ_1	-87.14	-0.003	-0.3
7	24.77	-25.69	θ_1	-46.0445	θ_1	-46.05	-0.0055	-0.55
8	-41.65	65.76	θ_1	-57.6513	θ_1	-57.65	0.0013	0.13
9	-60.48	-49.01	θ_1	39.0196	θ_1	39.02	0.0004	0.04
10	-37.99	-67.95	θ_1	60.791	θ_1	60.79	-0.001	-0.1

First configuration for determining θ_2, θ_3, and θ_4

The first configuration for the conducted experiments to find the joint angles at joint 2 to joint 4 took place when the wrist joint of the robot was located above the shoulder joint as featured in Figure 7. By implementing the developed inverse kinematics method, identical end-effector positions from the robot have been used in MATLAB simulation and the results were recorded.

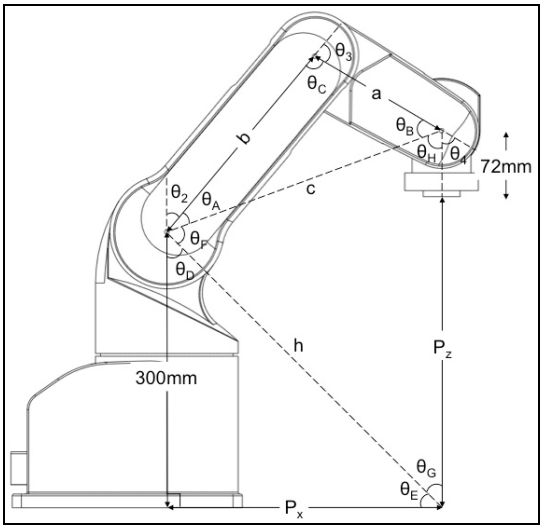

Figure 7: RV-2AJ robot at first configuration.

The comparison between the simulation and experimental results are presented in Table 4. The average error for θ_2, θ_3, and θ_4 over the 10 data readings are 0.34%, 0.82%, and 2.28% respectively.

Table 4: Comparison between simulation and experimental results for first configuration.

No. of test	*Pz* (mm)	Simulation (degree)		Experiment (degree)		Difference (degree)	Error (%)
1	397.35	θ_2	35.7386	θ_2	35.73	-0.0086	-0.86
		θ_3	66.3738	θ_3	66.39	0.0162	1.62
		θ_4	77.8877	θ_4	77.86	-0.0277	-2.77
2	387.34	θ_2	36.3252	θ_2	36.32	-0.0052	-0.52
		θ_3	68.9218	θ_3	68.93	0.0082	0.82
		θ_4	74.753	θ_4	74.73	-0.023	-2.3
3	377.35	θ_2	37.0279	θ_2	37.02	-0.0079	-0.79
		θ_3	71.2709	θ_3	71.28	0.0091	0.91
		θ_4	71.7012	θ_4	71.67	-0.0312	-3.12
4	367.35	θ_2	37.84	θ_2	37.84	0	0
		θ_3	73.4453	θ_3	73.45	0.0047	0.47
		θ_4	68.7147	θ_4	68.69	-0.0247	-2.47

5	357.35	θ_2	38.7597	θ_2	38.76	0.0003	0.03
		θ_3	75.443	θ_3	75.45	0.007	0.7
		θ_4	65.7973	θ_4	65.78	-0.0173	-1.73
6	347.36	θ_2	39.7787	θ_2	39.78	0.0013	0.13
		θ_3	77.2742	θ_3	77.28	0.0058	0.58
		θ_4	62.947	θ_4	62.93	-0.017	-1.7
7	337.34	θ_2	40.8968	θ_2	40.89	-0.0068	-0.68
		θ_3	78.9515	θ_3	78.96	0.0085	0.85
		θ_4	60.1518	θ_4	60.13	-0.0218	-2.18
8	327.36	θ_2	42.1013	θ_2	42.1	-0.0013	-0.13
		θ_3	80.4676	θ_3	80.48	0.0124	1.24
		θ_4	57.4311	θ_4	57.41	-0.0211	-2.11
9	317.37	θ_2	43.3936	θ_2	43.39	-0.0036	-0.36
		θ_3	81.8342	θ_3	81.84	0.0058	0.58
		θ_4	54.7721	θ_4	54.75	-0.0221	-2.21
10	307.35	θ_2	44.7725	θ_2	44.77	-0.0025	-0.25
		θ_3	83.0556	θ_3	83.06	0.0044	0.44
		θ_4	52.1719	θ_4	52.15	-0.0219	-2.19

Second configuration for determining θ_2, θ_3, and θ_4

For the second configuration experiment, the wrist joint of the robot was placed horizontally equal to the shoulder joint. By realizing this Cartesian position of the robot, the robot configuration in Figure 8 was achieved.

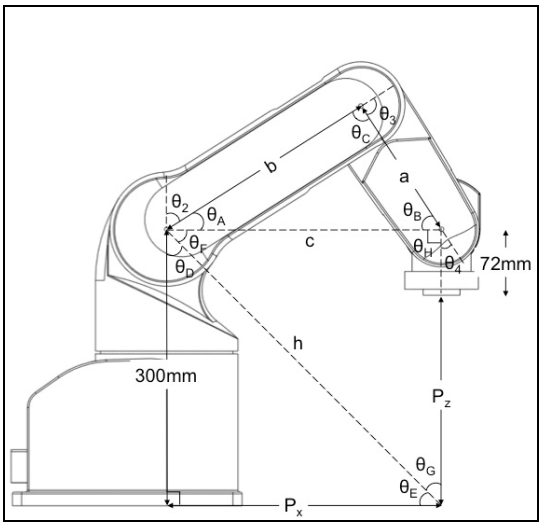

Figure 8: RV-2AJ robot at second configuration.

The simulation and experiment results from this particular position are presented in Table 5. The error produced for θ_2, θ_3, and θ_4 are 0.40%, 1.24%, and 1.84% respectively.

Table 5: Comparison between simulation and experimental results for second configuration.

Pz (mm)	Simulation (degree)		Experiment (degree)		Difference (degree)	Error (%)
300	θ_2	45.8340	θ_2	45.83	-0.0040	-0.40
	θ_3	83.8576	θ_3	83.87	0.0124	1.24
	θ_4	50.3084	θ_4	50.29	-0.0184	-1.84

Third configuration for determining θ_2, θ_3, and θ_4

The wrist joint of the robot was assigned to be lower than the shoulder joint for the third configuration. Detail posture of the robot is given in Figure 9.

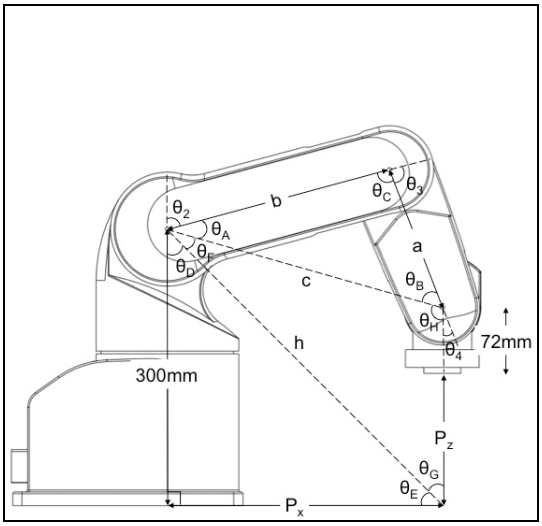

Figure 9: RV-2AJ robot at third configuration.

The results for the third region data readings between the MATLAB simulation and experiment are compared in Table 6. The average error for θ_2, θ_3, and θ_4 readings are 0.17%, 0.45%, and 1.49% respectively.

Table 6: Comparison between simulation and experimental results for third configuration.

No. of test	*Pz* (mm)	Simulation (degree)		Experiment (degree)		Difference (degree)	Error (%)
1	297.35	θ_2	46.2268	θ_2	46.22	-0.0068	-0.68
		θ_3	84.1273	θ_3	84.14	0.0127	1.27
		θ_4	49.6459	θ_4	49.63	-0.0159	-1.59
2	287.36	θ_2	47.7548	θ_2	47.75	-0.0048	-0.48
		θ_3	85.048	θ_3	85.05	0.002	0.2
		θ_4	47.1972	θ_4	47.18	-0.0172	-1.72
3	277.36	θ_2	49.3517	θ_2	49.35	-0.0017	-0.17
		θ_3	85.8292	θ_3	85.83	0.0008	0.08
		θ_4	44.8192	θ_4	44.8	-0.0192	-1.92
4	267.38	θ_2	51.0099	θ_2	51.01	1E-04	0.01
		θ_3	86.4649	θ_3	86.47	0.0051	0.51
		θ_4	42.5253	θ_4	42.51	-0.0153	-1.53
5	257.36	θ_2	52.7349	θ_2	52.73	-0.0049	-0.49
		θ_3	86.959	θ_3	86.96	0.001	0.1

		θ_4	40.3061	θ_4	40.29	-0.0161	-1.61
6	247.37	θ_2	54.5104	θ_2	54.51	-0.0004	-0.04
		θ_3	87.3081	θ_3	87.31	0.0019	0.19
		θ_4	38.1816	θ_4	38.17	-0.0116	-1.16
7	237.34	θ_2	56.3442	θ_2	56.34	-0.0042	-0.42
		θ_3	87.5145	θ_3	87.52	0.0055	0.55
		θ_4	36.1412	θ_4	36.13	-0.0112	-1.12
8	227.35	θ_2	58.2175	θ_2	58.22	0.0025	0.25
		θ_3	87.5768	θ_3	87.58	0.0032	0.32
		θ_4	34.2057	θ_4	34.19	-0.0157	-1.57
9	217.34	θ_2	60.1371	θ_2	60.14	0.0029	0.29
		θ_3	87.4956	θ_3	87.5	0.0044	0.44
		θ_4	32.3673	θ_4	32.35	-0.0173	-1.73
10	207.36	θ_2	62.0894	θ_2	62.09	0.0006	0.06
		θ_3	87.2716	θ_3	87.28	0.0084	0.84
		θ_4	30.639	θ_4	30.63	-0.009	-0.9

Comparison with other method

To compare the accuracy of the developed inverse kinematic model, another conventional method of using inverse matrix multiplication (Niku, 2011) has been established and the results are shown in Table 7. For this comparison, θ_{234} represents the total summation of θ_2, θ_3 and θ_4 which should theoretically produced 180°. Based on these findings, it is clear that the method discussed in this paper is more accurate.

Table 7: Comparison between Pythagoras's simulation and inverse matrix simulation results.

No. of test	*Pz* (mm)	Pythagoras's Simulation (degree)		Inverse Matrix Simulation (degree)	
1	277.36	θ_{234}	180.00	θ_{234}	179.9828
2	287.36	θ_{234}	180.00	θ_{234}	179.9828
3	297.35	θ_{234}	180.00	θ_{234}	179.9885
4	300.00	θ_{234}	180.00	θ_{234}	179.9885
5	307.35	θ_{234}	180.00	θ_{234}	179.9828
6	317.37	θ_{234}	179.99	θ_{234}	179.9828
7	327.36	θ_{234}	180.00	θ_{234}	179.9885

CONCLUSION

In this paper, the inverse kinematic equations for the joint angle of the RV-2AJ industrial robot arm with regards to the end-effector position have been derived. It can be seen that the developed inverse kinematics solution provides approximately 97.72% to 99.83% accuracy identical to the robot itself. On the other hand, the errors produced from the conducted experiments (when compared to the simulations) were possibly because of the robot calibration issue and mechanical properties that contributes to slightly false data readings whenever the robot arms were moved.

ACKNOWLEDGEMENT

This work was supported by Ministry of Education and Universiti Tun Hussein Onn Malaysia under Research Acculturation Grant Scheme Vot R032.

REFERENCE

Coman, M., Balan, R., Donca, R., & Verdeş, D. (2011). Optimization of the Control for the RV-2AJ Serial Robot. *Romanian Review Precision Mechanics, Optics and Mechatronics*, (39), 149–152. Retrieved from http://www.incdmtm.ro/editura/documente/pag. 149-152 COMEFIM 10 COMAN.pdf

Coman, M., Stan, S., Manic, M., & Balan, R. (2009). Design, Simulation and Control in Virtual Reality of a RV-2AJ Robot. In *2009 35th Annual Conference of IEEE Industrial Electronics* (pp. 2026–2031). IEEE. doi:10.1109/IECON.2009.5414922

Esa, M. F. M., Ibrahim, H., Mustaffa, N. H., & Majid, H. A. (2011). The Mitsubishi MelfaRxm middleware and application: A case study of RV-2AJ robot. In *2011 IEEE Conference on Sustainable Utilization and Development in Engineering and Technology (STUDENT)* (pp. 138–143). IEEE. doi:10.1109/STUDENT.2011.6089341

Haklidir, M., & Tasdelen, I. (2009). Modeling, simulation and fuzzy control of an anthropomorphic robot arm by using Dymola. *Journal of Intelligent Manufacturing*, *20*(2), 177–186. doi:10.1007/s10845-008-0227-9

Mitsubishi Electric. (2002). MELFA Industrial Robots - Specifications Manual.

Mitsubishi Electric. (2009). MELFA Industrial Robots. Consistent Quality - Precise Control.

Niku, S. B. (Saeed B. (2011). Introduction to robotics : analysis, control, applications. Hoboken, NJ: Wiley.

Šljivo, D. (2013). SIMULATION OF A 5-AXIS RV-2AJ ROBOT. *17th International Research/Expert Conference, "Trends in the Development of Machinery and Associated Technology"*, (September). Retrieved from http://tmt.unze.ba/zbornik/TMT2013/098-TMT13-096.pdf